Polarization-insensitive, 40 Gb/s wavelength and RZ-OOK-to-RZ-BPSK modulation format conversion by XPM in a highly nonlinear PCF

W. Astar[1*, 2], C.-C. Wei[1, 2, 3], Y.-J. Chen[2], J. Chen[3], and G. M. Carter[1, 2]

[1]*The Laboratory for Physical Sciences (LPS), 8050 Greenmead Drive, College Park, MD 20740, USA*
[2]*Department of Computer Science and Electrical Engineering, University of Maryland Baltimore County (UMBC), 1000 Hilltop Circle, Baltimore, MD 21250, USA*
[3]*Institute of Electro-Optical Engineering and Department of Photonics, National Chiao Tung University, 1001 Ta Hsueh Rd., Hsin-Chu, Taiwan, 300*
**Corresponding author: notilos@lps.umd.edu*

Abstract: Polarization-insensitive wavelength conversion, as well as the conversion of return-to-zero (RZ) ON-OFF keying (RZ-OOK) to RZ binary phase-shift keying (RZ-BPSK), has been simultaneously achieved at 40 Gb/s for the first time by cross-phase modulation (XPM) in a highly birefringent, nonlinear photonic crystal fiber (PCF). A 10^{-9}-BER receiver sensitivity conversion penalty of < 3 dB was achieved for a polarization scrambled, 40 Gb/s 25%-RZ-OOK pump, when the 40 Gb/s RZ probe was launched at 45^{o} with respect to the birefringence axes of the PCF and when the pump-probe detuning was greater than about 6 nm.

OCIS codes: (060.5060) Phase modulation; (190.4370) Nonlinear optics, fibers; (260.1440) Birefringence; (230.7405) Optical devices, wavelength conversion devices

References and links

1. K. Mishina, A. Maruta, S. Mitani, T. Miyahara, K. Ishida, K. Shimizu, T. Hatta, K. Motoshima, and K.-I. Kitayama, "NRZ-OOK-to-RZ-BPSK modulation-format conversion using SOA-MZI wavelength converter," J. Lightwave Technol. **24**, 3751-3758 (2006).
2. W. Astar, A. S. Lenihan, and G. M. Carter, "Performance of DBPSK in a 5 × 10 Gb/s mixed modulation format Raman/EDFA WDM system," IEEE Photon. Technol. Lett. **17**, 2766-2768 (2005).
3. W. Astar and G. M. Carter, "10 Gbit/s RZ-OOK to RZ-BPSK format conversion using SOA and synchronous pulse carver" Electron. Lett. **44**, 369 -370 (2008).
4. K. Mishina, S. Kitagawa, and A. Maruta, "All-optical modulation format conversion from on-off-keying to multiple-level phase-shift-keying based on nonlinearity in optical fiber," Opt. Express **15**, 8444-8453 (2007), http://www.opticsexpress.org/abstract.cfm?uri=OE-15-13-8444.
5. C. D. Poole, "Measurement of polarization-mode dispersion in single-mode fibers with random mode coupling," Opt. Lett. **14**, 523-525 (1989).
6. K. P. Hansen, J. R. Folkenberg, C. Peurecheret, and A. Bjarklev, "Fully dispersion controlled triangular-core nonlinear photonic crystal fiber," in *Conf. Proc. of Optical Fiber Communication (OFC)*, 2003, paper PD2-1.
7. A. S. Lenihan, R. Salem, T. E. Murphy, G. M. Carter, "All-optical 80-Gb/s time-division demultiplexing using polarization-insensitive cross-phase modulation in photonic crystal fiber," IEEE Photon. Technol. Lett. **18**, 1329-1331 (2006).
8. B. L. Heffner, "Automated measurement of polarization mode dispersion using Jones matrix eigenanalysis," IEEE Photon. Technol. Lett. **14**, 1066-1068 (1992).
9. K. K. Chow, C. Shu, C. Lin, and A. Bjarklev, "Polarization-insensitive widely tunable wavelength converter based on four-wave mixing in a dispersion-flattened nonlinear photonic crystal fiber," IEEE Photon. Technol. Lett. **17**, 624-626 (2005).
10. J. H. Lee, W. Belardi, K. Furusawa, P. Petropoulos, Z. Yusoff, T. M. Monro, and D. J. Richardson, "Four-wave mixing based 10-Gb/s tunable wavelength conversion using a holey fiber with a high SBS threshold," IEEE Photon. Technol. Lett. **15**, 440-442 (2003).
11. K. Inoue, "Polarization independent wavelength conversion using fiber four-wave mixing with two orthogonal pump lights of different frequencies," J. Lightwave Technol. **12**, 1916-1920 (1994).

#96419 - $15.00 USD Received 20 May 2008; revised 15 Jul 2008; accepted 22 Jul 2008; published 28 Jul 2008

12. T. Tanemura, J. Suzuki, K. Katoh, and K. Kikuchi, "Polarization-insensitive all-optical wavelength conversion using cross-phase modulation in twisted fiber and optical filtering," IEEE Photon. Technol. Lett. **17**, 1052-1054 (2005).
13. T. Hasegawa, K. Inoue, and K. Oda, "Polarization independent frequency conversion by fiber four-wave mixing with a polarization diversity technique," IEEE Photon. Technol. Lett. **5**, 947-949 (1993).
14. T. Yang, C. Shu, and C. Lin, "Depolarization technique for wavelength conversion using four-wave mixing in a dispersion-flattened photonic crystal fiber," Opt. Express **13**, 5409-5415 (2005), http://www.opticsinfobase.org/abstract.cfm?URI=oe-13-14-5409.
15. A. S. Lenihan, and G. M. Carter, "Polarization-insensitive wavelength conversion at 40 Gb/s using birefringent nonlinear fiber," in *Conf. Proc. of Conference on Lasers and Electro-Optics (CLEO)*, 2007, paper CThAA2.
16. S. Kumar, A. Selvarajan, and G. Anand, "Nonlinear propagation of two optical pulses of two different frequencies in birefringent fibers", J. Opt. Soc. Am. *B* **11**, 810-817 (1994).
17. G. P. Agrawal, *Nonlinear Fiber Optics* (Academic Press, 2001), pp. 238-277.
18. C. R. Menyuk, "Nonlinear pulse-propagation in birefringent optical fiber," IEEE J. Quantum Electron. **23**, 174-176 (1987).
19. P. J. Winzer, and H. Kim, "Degradations in Balanced DPSK Receivers," IEEE Photon. Technol. Lett. **15**, 1282-1284 (2003).
20. N. Sugimoto, T. Nagashima, T. Hasegawa, S. Ohara, and K. Taira and K. Kikuchi, "Bismuth-based optical fiber with nonlinear coefficient of 1360 $W^{-1}km^{-1}$," in *Conf. Proc. of Optical Fiber Communication (OFC)*, 2003, paper PDP26.

1. Introduction

Wavelength conversion may be used to facilitate the full utilization of the bandwidths of fibers deployed in dense wavelength division multiplexed (DWDM) networks, as well as to minimize network blocking probability, and to enhance network interoperability. As some networks have been upgraded from RZ-OOK to RZ-differential phase-shift keying (RZ-DPSK) due to the latter's 3-dB optical signal-to-noise ratio (OSNR) advantage as well as its superior performance in DWDM transmission, interoperability with other networks still carrying RZ-OOK can lead to mixed-modulation format transmission over the long-haul back-bone [1]. OOK/DPSK mixed-modulation format transmission has been found to be highly deleterious to the DPSK channels due to the XPM-mediated, power-phase conversion of the pattern-dependent OOK channels [2]. The OOK/DPSK transmission incompatibility has consequently motivated the need to explore simultaneous wavelength and OOK-to-BPSK modulation format conversion in the cross-connects (or gateways) interfacing metropolitan/wide-area networks with the long-haul back-bone [1]. Mishina *et al.* [1] were the first to demonstrate 10 Gb/s wavelength and OOK-to-BPSK format conversion in semiconductor optical amplifiers (SOAs) configured in a Mach-Zehnder interferometer (MZI), and demonstrated a receiver sensitivity gain of 3 dB relative to the OOK signal. More recently, Astar and Carter [3] demonstrated the first polarization-insensitive, 10 Gb/s wavelength and OOK-to-BPSK format conversion by XPM in a single saturated bulk SOA using only commercially available components, and achieving a receiver sensitivity gain of 1.5 dB. Although format conversion techniques using SOAs are attractive as they are amenable to single-chip integration, they can also be problematic for the resultant BPSK signal. To mitigate pattern-dependence and chirp, Mishina *et al.* [1] required the use of CW assist light; while the single SOA approach [3] also suffered due to residual cross-gain modulation, as well as pattern-dependence due to the slow (> 100 ps) response time of the bulk SOA, and which is transferred to the phase of the BPSK signal.

Simultaneous wavelength and OOK-to-*M*-PSK format conversion has also been explored in a highly nonlinear fiber (HNLF), which takes advantage of the ultra-fast (~ fs) $\chi^{(3)}$-effect. Being a fiber-based approach also makes it suitable for integration with fiber-based systems. Mishina *et al.* [4] have demonstrated wavelength, and OOK-to-BPSK, and (2 × OOK)-to-quadrature-phase-shift-keying at 10.7 Gb/s in a 100-m-long, non-birefringent HNLF, which had a nonlinear coefficient of 24 $W^{-1}km^{-1}$. However, the efficacy of the technique for arbitrarily polarized OOK signals, a critical consideration since the signal state-of-polarization

#96419 - $15.00 USD Received 20 May 2008; revised 15 Jul 2008; accepted 22 Jul 2008; published 28 Jul 2008

(SOP) varies unpredictably in installed fiber plants, was neither analyzed nor experimentally investigated. Recent advances in the design and fabrication of nonlinear fiber have resulted in short PCF for which the birefringent axes remain fixed over the entire length. The commercially available PCF (NL·1550·NEG·1 by Crystal Fibre A/S) used here falls into this category, and was confirmed experimentally using the fixed-analyzer technique of Poole [5]. The transmitted power output by the analyzer varied periodically as seen in Fig. 1, which

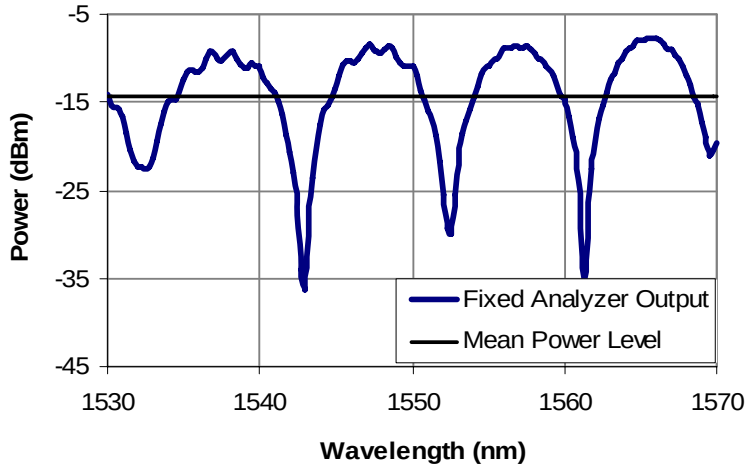

Fig. 1. Fixed-analyzer transmission spectrum showing periodic behaviour, and indicating that the PCF is in the short coupling length regime.

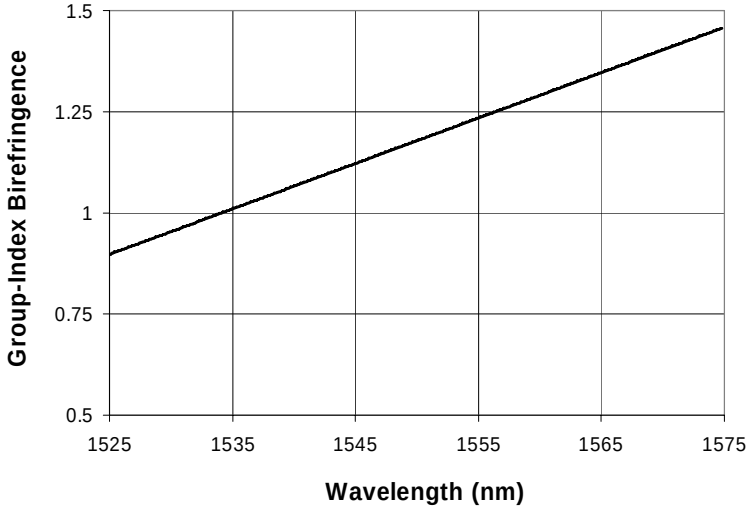

Fig. 2. Measured group-index birefringence ($\times 10^{5}$) of PCF using the Jones Matrix Eigenanalysis Method.

confirms that the length of the PCF is shorter than its birefringence coupling length, or that the birefringence axes remain fixed over its entire physical length. The PCF can therefore be effectively treated as a single waveplate. PCFs can also exhibit a relatively large group-index birefringence, in the range of 10^{-5}-10^{-4} [6]. For this type of PCF, it has been verified [7] to exceed 10^{-5} for wavelengths > 1535 nm using the Jones Matrix Eigenanalysis Method [8]. The

#96419 - $15.00 USD Received 20 May 2008; revised 15 Jul 2008; accepted 22 Jul 2008; published 28 Jul 2008

PCF birefringence is also wavelength dependent, varying by as much as 25% over the C-band, as shown in Fig. 2. The PCF has also been found to exhibit a nearly flat dispersion profile (with dispersion slope of ~ 10^{-3} ps/nm^{2}km), a high nonlinear coefficient (γ) of ~ 11 W^{-1}km^{-1}, a low propagation loss of 0.008 dB/m, and a high stimulated Brillouin scattering threshold of ~ 22 dBm for lengths < 100 m, and a continuous wave (CW) pump [9]. Furthermore, the PCF's normal dispersion profile, with dispersion < -1 ps/nmkm over the C-band, ensures that modulation instability effects are avoided [10].

A serious drawback of pump-probe applications utilizing nonlinear fiber is the strong dependence of the $\chi^{(3)}$-effect on the SOPs of the pump and the probe. Apart from perfectly matching the SOPs of the pump and the probe over the length of the PCF, other techniques have been suggested to alleviate the polarization dependence of XPM: Using two cross-polarized pumps [11]; launching the pump circularly polarized in a spun, circularly birefringent fiber [12]; through polarization diversity [9, 13]; and by pump depolarization [14]. Another means of obtaining polarization insensitive operation is to utilize the birefringence of the nonlinear fiber itself, when possible. The technique proposed here is similar to that of [15] in which the CW pump was launched at 45^o relative to the birefringent axes of the PCF to mitigate the polarization sensitivity of wavelength conversion by XPM. However, a 45^o pump launch by itself is inadequate to compensate the polarization sensitivity of XPM, and also requires a minimum pump-probe detuning (PPD) as will be clarified in the ensuing section.

2. Principal of operation

The theory of pump-probe XPM in a highly birefringent fiber is well-understood [16]. The pump-probe interaction can be described by the vector nonlinear Schrodinger equation for the probe (A_2), under the assumption of negligible propagation loss, dispersion, and when the pump power is much greater than that of the probe,

$$\frac{dA_{2x}}{dz} = i\gamma\left(2\left|A_{1x}\right|^2 + \frac{2}{3}\left|A_{1y}\right|^2\right)A_{2x} + \frac{2i\gamma}{3}A_{1x}^{*}A_{1y}A_{2y}\exp\left[i\frac{z}{c}\sum(\omega B)\right] + \frac{2i\gamma}{3}A_{1x}A_{1y}^{*}A_{2y}\exp\left[-i\frac{z}{c}\Delta(\omega B)\right] \tag{1}$$

$$\frac{dA_{2y}}{dz} = i\gamma\left(2\left|A_{1y}\right|^2 + \frac{2}{3}\left|A_{1x}\right|^2\right)A_{2y} + \frac{2i\gamma}{3}A_{1y}^{*}A_{1x}A_{2x}\exp\left[-i\frac{z}{c}\sum(\omega B)\right] + \frac{2i\gamma}{3}A_{1y}A_{1x}^{*}A_{2x}\exp\left[i\frac{z}{c}\Delta(\omega B)\right] \tag{2}$$

where A_1 is the pump field, B is the phase-index birefringence (PIB), and

$$\sum(\omega B) = \omega_1 B_1 + \omega_2 B_2 \tag{3}$$

$$\Delta(\omega B) = \omega_1 B_1 - \omega_2 B_2 \quad . \tag{4}$$

The PIB may be obtained from the group-index birefringence (GIB) found from Fig. 2, as

$$\begin{cases} B = \dfrac{1}{\omega}\int G(\Omega)d\Omega \\ G(\Omega) = \alpha_G + \beta_G\dfrac{2\pi c}{\Omega} \quad . \end{cases} \tag{5}$$

where α_G (=1.625 × 10^{-4}) and β_G (=112) are fitting parameters used for Fig.2. It was experimentally established that the PCF is highly birefringent (Fig. 2), with GIB many orders of magnitude larger than that (~ 10^{-7}) of standard transmission fiber. Consequently, its beat length (L_B) would be much shorter than its physical length (L), or

#96419 - $15.00 USD Received 20 May 2008; revised 15 Jul 2008; accepted 22 Jul 2008; published 28 Jul 2008

$$\omega_j B_j \frac{L}{c} = 2\pi \frac{L}{L_{Bj}} > 2\pi, \tag{6}$$

so the first exponential term in Eqs. (1, 2) may be ignored [17, 18], as it rapidly oscillates within the length of the PCF, thus averaging out to a negligible value relative to the non-oscillatory terms. The other oscillatory term vanishes under the more stringent condition applied to Eq. (4),

$$\left|\omega_1 B_1 - \omega_2 B_2\right| \cdot \frac{L}{c} = 2\pi \left| \frac{L}{L_{B1}} - \frac{L}{L_{B2}} \right| > 2\pi \tag{7}$$

which assumes sufficient PPD for the condition to be met. Using Eq. (5), the above condition reduces to

$$(\omega_1 - \omega_2)\,\alpha_G - \beta_G \ln\left(\frac{\omega_1}{\omega_2}\right)^{2\pi c} > \frac{2\pi c}{L} \tag{8}$$

which may be recast in terms of wavelengths as

$$\alpha_G \,\Delta\left(\frac{1}{\lambda}\right) - \beta_G \ln\left(\frac{\lambda_2}{\lambda_1}\right) > \frac{1}{L}. \tag{9}$$

This equation can be further simplified if the minimum PPD required for polarization-insensitive XPM is assumed to be a small percentage of typical wavelengths involved: Using the differential approximation for the first term, and expanding the ln(·) second term to first order only allows an analytical solution to the problem,

$$\Delta\lambda > \frac{1}{L} \cdot \left(\frac{\alpha_G}{\lambda_1^2} - \frac{\beta_G}{\lambda_1} \right)^{-1} \tag{10}$$

and taking the PCF length to be 30 m, and the pump wavelength at 1553 nm, the PPD resolves to 7 nm, which is close to that observed in practice. The difference between the approximate Eq. (9) and the exact Eq. (10) is negligible.

The first terms on the RHS of Eqs. (1)-(2) responsible for the required phase shift show that large deviations from π would be expected if the pump ($\mathbf{A_1}$) is polarization-scrambled. The worst-case scenario occurs when the pump is aligned to one birefringent axis, while the probe happens to be aligned with the other. Such cases can be avoided by launching the probe at 45° relative to the birefringent axes, or equivalently, anywhere on the great circle of S_1=0 on the Poincaré sphere. When combined with Eq. (7), Eqs. (1)-(2) finally yield the desired expression for the RZ-BPSK signal at the output plane of the PCF:

$$\mathbf{A_2}(L,t) =$$
$$\left(\frac{P_2(0,t)}{2}\right)^{1/2} \left\{ \mathbf{x}\, e^{i\varphi_{2x}} \exp\left[2i\gamma L\left(P_{1x}(0,t) + \tfrac{1}{3}P_{1y}(0,t)\right)\right] + \mathbf{y}\, e^{i\varphi_{2y}} \exp\left[2i\gamma L\left(P_{1y}(0,t) + \tfrac{1}{3}P_{1x}(0,t)\right)\right] \right\} \tag{11}$$

and where the RZ-OOK pump is expressed as,

$$\mathbf{A}_1(L,t) = \mathbf{x}\, e^{i\varphi_{1x}} \sqrt{P_{1x}(0,t)} + \mathbf{y}\, e^{i\varphi_{1y}} \sqrt{P_{1y}(0,t)} = \sqrt{P_{10}} \left(\mathbf{x}\, e^{i\varphi_{1x}} \cos\psi_1 + \mathbf{y}\, e^{i\varphi_{1y}} \sin\psi_1 \right). \tag{12}$$

#96419 - $15.00 USD Received 20 May 2008; revised 15 Jul 2008; accepted 22 Jul 2008; published 28 Jul 2008

In Eq. (12), P_{10} (= $P_{1x}(0,t) + P_{1y}(0,t)$) is the input pump power, ψ_1 is the launch angle for the pump, and $\varphi_{1x,y}$ also carry the effects of SPM experienced by the pump during propagation.

It is observed in Eq. (11) that even when an unscrambled pump is launched orthogonal to the probe, some phase is still induced in the probe. Thus, it should be possible to affect modulation format conversion even for mutually orthogonal pump and probe, in principal. For this case however, as the induced phase is always one-third of that for the case of mutually parallel pump and probe, it would be significantly less efficient, i.e. much more demanding on the pump power (or equivalently, the pulse-width) required to achieve the desired π phase shift, given a specific PCF length: Assuming that a ($2\gamma LP_{10}$ =) π phase shift for mutually parallel pump and probe on the same birefringent axis is supported by the experimental parameters, launching the same pump and probe to the two orthogonal birefringent axes would result in the drastically smaller $\pi/3$ phase shift. For a scrambled pump and 45^o probe launch, the weaker $\pi/3$ phase shift is unavoidable, and its presence in addition to the desired phase shift will lead to some penalty.

It is also observed from (11) that the XPM-induced phase is not flat over a bit-slot of the probe, but carries the profile of the pump pulse power. However, as long as the pump pulse decays significantly slower than the probe pulse, the induced phase will be close to flat over the duration of a probe pulse.

3. Experimental results and discussion

To carry out RZ-OOK-to-RZ-BPSK format conversion in PCF, a pump-probe configuration was employed in which the pump was a wavelength-tunable, 40 Gb/s, 2^{31}-1 pseudo-random bit sequence; and the probe, a 40 Gb/s optical clock fixed at 1553 nm (Fig. 3). The RZ-OOK pump pulses were ~ 6 ps full-width-at-half-maximum (FWHM), generated using a Franz-Keldysh electroabsorption modulator reverse-biased at -2 V, driven at 4 V_{pp}, and fed with a CW laser. The probe pulses were generated using an actively mode-locked GaInAsP/InP laser diode, and were 2-ps FWHM, transform-limited hyperbolic secant pulses. The SOP of the pump was controlled by either a polarization scrambler (PS) or a mechanical polarization

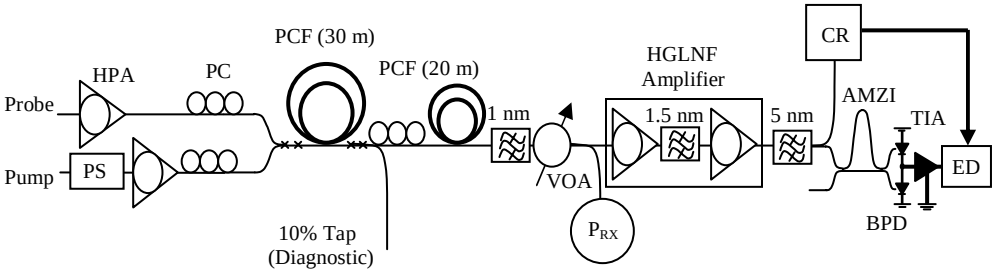

Fig. 3. RZ-OOK-to-RZ-BPSK format conversion experimental set-up (HPA: high-power amplifier; VOA: variable optical attenuator; P_{RX}: receiver power; CR: clock recovery; AMZI: asymmetric Mach-Zehnder interferometer, BPD: balanced photodetector; TIA: transimpedance amplifier; ED: error detector).

controller (PC) while that of the probe was controlled solely by a PC. The average powers of the pump and the probe were estimated to be 24 dBm, and 13 dBm. The probe power was governed by a trade-off between maximum output OSNR, and SPM-induced spectral broadening which caused distortion due to receiver filtering. To enhance the XPM-induced phase-shift, a second, 20-m-long PCF spool was used. A PC intermediate to the two spools was used to ensure proper launch conditions into the second spool. At the output, the probe was isolated using a 1-nm thin-film optical bandpass filter (OBPF), and that was followed by a dual-stage, high-gain, low-noise-figure (HGLNF) optical amplifier that carried an inter-stage, 1.5-nm OBPF. Another 5-nm filter was used at the amplifier output to reduce the

#96419 - $15.00 USD Received 20 May 2008; revised 15 Jul 2008; accepted 22 Jul 2008; published 28 Jul 2008

accumulated noise. The rest of the standard DPSK receiver consisted of OC-768 clock recovery, 25-ps-delay AMZI, 40 Gb/s BPD, and a 40 Gb/s TIA. The average power input to each detector was about 6 dBm. Baseline receiver sensitivity measurements for RZ-OOK were carried out using a single detector in the BPD, with the AMZI bypassed.

To characterize the sensitivity of XPM induced in the probe as a function of PPD, a 1553 nm CW laser was used as the probe, and a 0.5-nm OBPF was detuned to the blue side of the XPM-induced pedestal in the probe, at the output of the 20-m PCF spool. The resultant signal was wavelength-converted 40 Gb/s RZ-OOK. For this experiment, the probe was launched at 45^{o} with respect to the PCF birefringence axes of the 30-m PCF spool, while the SOP of the RZ-OOK pump was swept over the Poincaré sphere through the pump PC. Use of the CW probe and blue-shifting the filter relative to the probe carrier at the output minimized cross-talk complications that would arise with the use of the broadband 2-ps-pulsed probe for PPD as small as 1 nm. An optical spectrum analyzer set in minimum-maximum (min-max) power mode was used to characterize the power fluctuations in the output probe while the pump SOP was varied. Power fluctuation as a function of PPD is seen in Fig. 4, which demonstrates that a minimum PPD of ~ 6 nm is required to minimize the power fluctuation in the probe below 1 dB. Beyond the first minimum, the power fluctuation is seen to be no more than 1 dB larger, and gets progressively smaller at larger PPD.

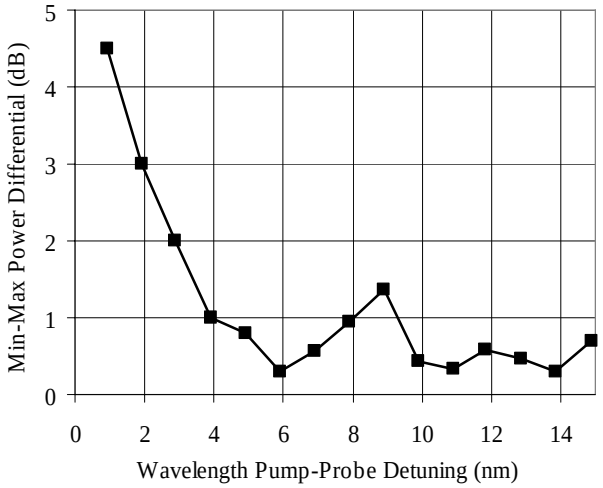

Fig. 4. Power fluctuation observed in the probe spectrum as a function of PPD.

To carry out receiver sensitivity experiments on the RZ-BPSK signal generated in the PCF, the PPD was set to 6 nm (corresponding to pump at 1547 nm). The 40 Gb/s RZ-OOK pump was polarization-scrambled, and a 45^{o}-launch was used for the pulsed probe. The results are shown in Fig. 5. For the case of ◊, the RZ-BPSK probe demonstrated a < 3 dB penalty relative to baseline RZ-OOK (×) which is partly attributed to deviations from π in the XPM-induced phase shift as the RZ-OOK pump is polarization scrambled (Eq. (11)). For baseline RZ-OOK, the mode-locked laser diode was used as the pulsed source. When the pump scrambler was turned off while the probe was still in 45^{o}-launch, the receiver sensitivity of RZ-BPSK varied by an order of 1 dB as the pump SOP was mechanically swept over the Poincaré sphere using the pump PC. While the pump was scrambled, the probe PC was adjusted for highest BER (corresponding to launch along a birefringent axis) and maximum RZ-BPSK eye-diagram degradation. For this case (Δ), receiver sensitivity exhibited an error

#96419 - $15.00 USD Received 20 May 2008; revised 15 Jul 2008; accepted 22 Jul 2008; published 28 Jul 2008

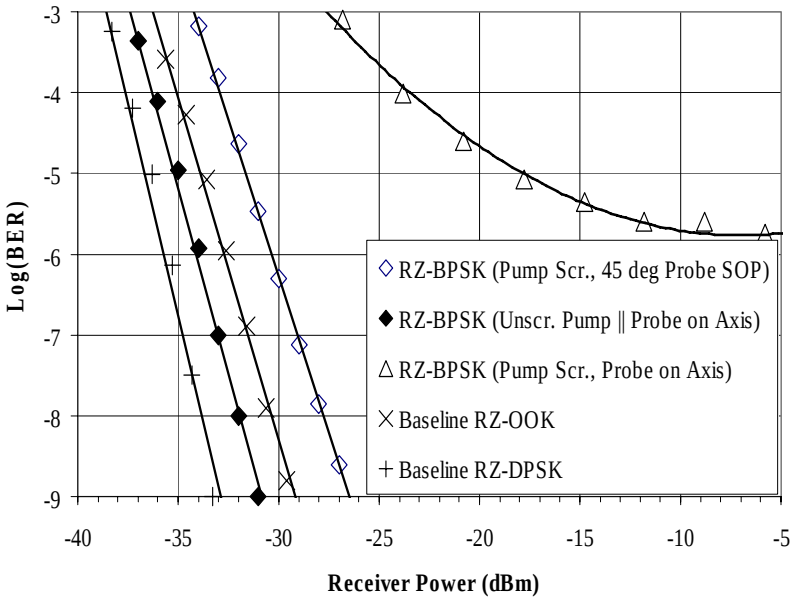

Fig. 5. Receiver sensitivity measurement results for 6 nm PPD.

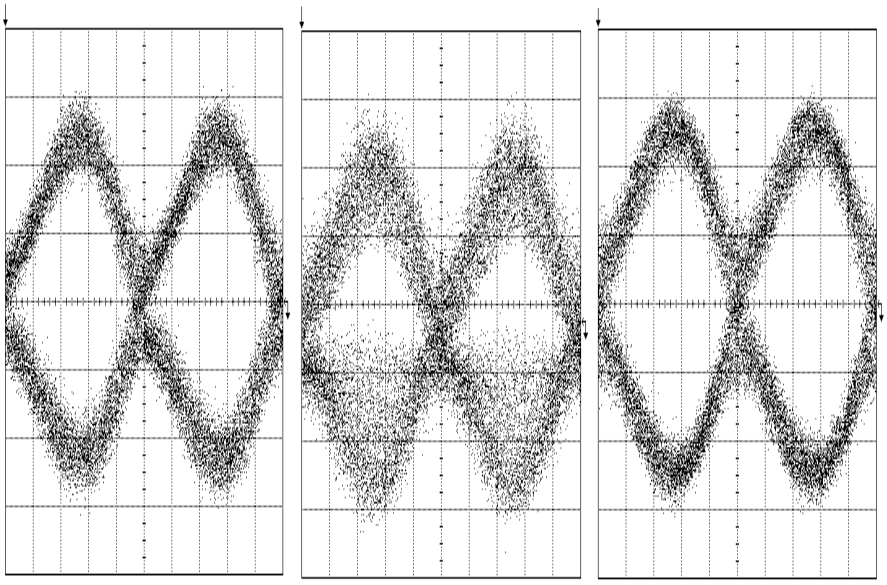

(a) (b) (c)

Fig. 6. RZ-BPSK probe eye-diagrms for PPD of 6 nm and OSNR of 18.5 dB/1nm: (a) Pump scrambled (45° probe launch); (b) Pump scrambled (probe on an axis); (c) Same as (b) but with unscrambled pump aligned to probe.

floor. However, when the scrambler was turned off, and the pump PC was adjusted for best RZ-BPSK probe eye-diagram opening, the RZ-BPSK probe for this case demonstrated a ~ -2 dB penalty relative to baseline RZ-OOK, and ~ 2 dB penalty relative to baseline RZ-

#96419 - $15.00 USD Received 20 May 2008; revised 15 Jul 2008; accepted 22 Jul 2008; published 28 Jul 2008

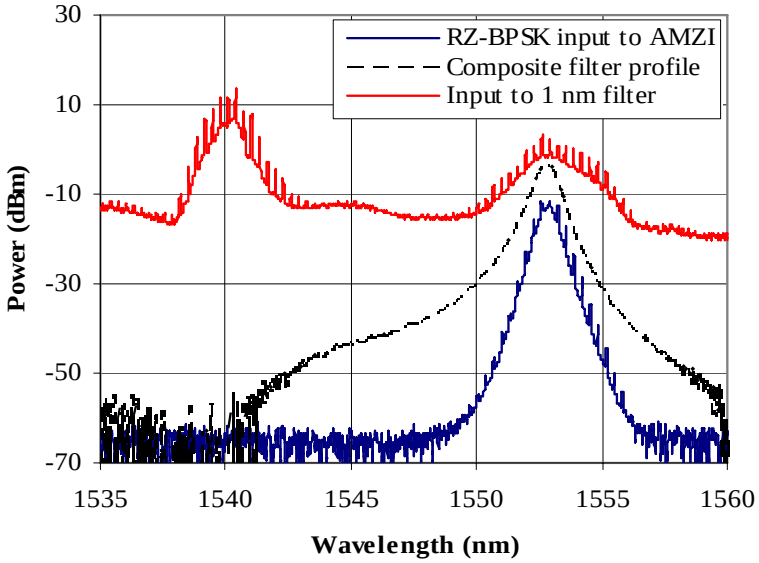

Fig. 7. Spectra obtained at a resolution bandwidth of 0.05 nm, and for a PPD of >10 nm. The traces have been offset relative to each other for clarity.

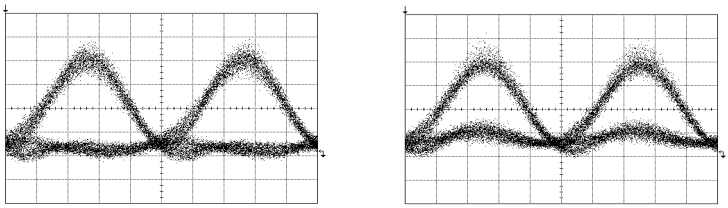

(a) (b)

Fig. 8. AMZI output port eye-diagrams for a PPD of 6 nm, OSNR of 18.5 dB/1nm, and pump and probe aligned to same birefringent axis: (a) Alternate mark inversion signal; (b) Duobinary signal.

DPSK(+) (which also used the mode-locked laser diode as its pulsed-source). The last result is independent of PPD, and all the results are also qualitatively reflected in the receiver eye-diagrams (Fig. 6). This experiment was repeated at other pump wavelengths lower than 1547 nm, and the resultant receiver sensitivity curves (not shown) were all within a dB better than those seen in Fig. 5 due to output OSNR variations in the probe, as neither of the HPAs in Fig. 3 was gain-flattened. No measurements were carried out for PPD < 3 nm due to a large cross-talk produced by the SPM-broadened pump, exacerbated by the broad 1-nm OBPF used at the output of the PCF, and which was required for the broadband 2-ps pulse used for the probe. Typical spectra at various locations in the set-up (Fig. 3) are also seen in Fig. 7.

It should be stated that although a second, 20-m PCF spool was utilized in the experiment to enhance the nonlinearity, the minimum PPD was found to be governed by the 30-m PCF. This is due to the fact that the length of the 20-m PCF spool is a factor 2/3- smaller than that of the 30-m PCF. Further, the power at the input of the 20-m PCF was significantly smaller than that at the input of the 30-m PCF due to the use of a diagnostic tap, and two SMF/PCF mode adapters at ~ 1 dB loss/adapter. Consequently, the nonlinear phase-shift due to the 20-m PCF spool was substantially smaller than that produced in the 30-m PCF spool.

#96419 - $15.00 USD Received 20 May 2008; revised 15 Jul 2008; accepted 22 Jul 2008; published 28 Jul 2008

Some of the penalties observed for the RZ-BPSK probe were somewhat large. For unscrambled pump and probe aligned to the same axis (solid diamonds, Fig. 5) for instance, the penalty was close to 2 dB (compared to baseline RZ-DPSK). The penalty is ascribed to an insufficient nonlinear phase shift, which was easily deduced by lowering the pump power on the pump HPA in Fig. 3, and is also reflected in the outputs of the AMZI (Fig. 8). Although the alternate-mark inversion (AMI) signal is of high quality, the duobinary signal demonstrates rail distortion, and it was pointed out by Winzer [19] that the duobinary signal is much more sensitive than its AMI counterpart to phase imperfections in the RZ-BPSK signal. A computation using experimental parameters revealed that the induced nonlinear phase shift was about 2.4 radians for pump and probed launched along the same birefringent axis, so that better results should be obtainable with a longer PCF or a higher pump power (or a combination there-of) that would ensure a nonlinear phase shift of π radians, since the length of the PCF used was not optimized for the application (for the maximum available pump power.) Given a length of PCF, it is simpler to merely raise the pump power (if possible) till the ZERO rail in the duobinary signal (Fig. 8(b)) is completely flattened, which should consequently lower the receiver sensitivity penalty for the resultant RZ-BPSK signal to something negligible (relative to baseline RZ-DPSK). This should also lower the penalty for the polarization-scrambled pump case. Nevertheless, the experiment reported demonstrates that at least in principal, polarization-insensitive modulation format conversion is feasible in PCF without the use of depolarization techniques or polarization diversity.

Although the PCF used was obviously not optimized for modulation format conversion, some conclusions may be made about the properties of a fiber best-suited for this application. Recent advances in nonlinear fiber fabrication have made possible fibers with nonlinear coefficients in excess of 1000 $W^{-1}km^{-1}$ (recently, a Bi_2O_3-based glass fiber demonstrated a nonlinear coefficient > 1300 $W^{-1}km^{-1}$ [20]). For polarization-insensitive modulation format conversion, the nonlinear fiber should possess a very high birefringence of order 10^{-3} to reduce the minimum PPD to < 5 nm; a nonlinear coefficient of $\geq$ 2000 $W^{-1}km^{-1}$ to enhance the nonlinear phase shift, thereby reducing the fiber length; a low propagation loss of < 50 dB/km, and a low coupling loss of < 1 dB to standard single-mode fiber. The fiber in question should also possess a fairly flattened, normal dispersion coefficient (D) > -30 ps/nmkm, as well as a low dispersion-slope coefficient of ($|S|$) <0.1 ps/nm^2km over the spectral (S-, C-, or L-) band of interest, both cogent considerations for high ($\leq$ 40Gb/s) data-rate applications. Moreover, these characteristics should be isotropic (polarization-independent) over the length of the short fiber as for the PCF examined, and fairly spectrally invariant over the spectral region of interest. Assuming a realistic 50% duty cycle for the RZ-OOK pulse, these fiber properties would enable OOK-to-BPSK format conversion in a short (~ 10 m) fiber, with a modest pump power requirement (~ 10 dBm) readily achievable with commercial WDM amplifiers.

4. Summary and conclusions

Polarization-insensitive, simultaneous wavelength and RZ-OOK-to-RZ-BPSK modulation format conversion has been demonstrated for the first time at 40 Gb/s in a highly birefringent PCF. It was theoretically and experimentally found that a 45^o probe launch by itself is inadequate to mitigate polarization sensitivity in the probe, but also required a minimum pump-probe detuning of ~ 6 nm. For RZ-OOK pump and probe launched along the same PCF birefringent axis, the output RZ-BPSK probe performed better than baseline RZ-OOK by ~ 2 dB, and worse than baseline RZ-DPSK by ~ 2 dB. When the pump scrambler was turned on, an error floor was observed in the receiver sensitivity curve for the probe, and the corresponding eye-diagram was severely degraded. However, once the probe was relaunched at 45^o with respect to the PCF birefringent axes, error-free BER was achieved with a sensitivity penalty of < 3 dB relative to baseline RZ-OOK. It should be possible to reduce this penalty to ~ 1 dB with a longer PCF and/or higher RZ-OOK pump power.

#96419 - $15.00 USD Received 20 May 2008; revised 15 Jul 2008; accepted 22 Jul 2008; published 28 Jul 2008

The modulation format conversion may be applicable to OOK/DPSK mixed-modulation format transmission [2], which was found to be deleterious to DPSK due to the XPM-mediated power-phase conversion of the pattern-dependent OOK channels. By converting the OOK channels to pattern-independent BPSK ones, the XPM impairment would be significantly mitigated. The technique described herein should be superior to that using bulk SOAs, which although relatively polarization-insensitive, suffers from pattern-dependence due to a large carrier lifetime, and XGM-induced distortion [4]. Format conversion in PCF on the other hand utilizes the ultra-fast $\chi^{(3)}$ effect, which eliminates pattern-dependent complications.

#96419 - $15.00 USD Received 20 May 2008; revised 15 Jul 2008; accepted 22 Jul 2008; published 28 Jul 2008